JOURNAL OF VIROLOGY, Mar. 2005, p. 3370–3381 Vol. 79, No. 6
0022-538X/05/$08.00+0 doi:10.1128/JVI.79.6.3370–3381.2005

Increased Epitope-Specific CD8$^+$ T Cells Prevent Murine Coronavirus Spread to the Spinal Cord and Subsequent Demyelination

Katherine C. MacNamara,[1] Ming Ming Chua,[1] Peter T. Nelson,[2] Hao Shen,[1] and Susan R. Weiss[1]*

Department of Microbiology[1] and Department of Pathology and Laboratory Medicine,[2] School of Medicine, University of Pennsylvania, Philadelphia, Pennsylvania

Received 17 August 2004/Accepted 2 November 2004

CD8$^+$ T cells are important for clearance of neurotropic mouse hepatitis virus (MHV) strain A59, although their possible role in A59-induced demyelination is not well understood. We developed an adoptive-transfer model to more clearly elucidate the role of virus-specific CD8$^+$ T cells during the acute and chronic phases of infection with A59 that is described as follows. C57BL/6 mice were infected with a recombinant A59 virus expressing the gp33 epitope, an H-2D^b-restricted CD8$^+$ T-cell epitope encoded in the glycoprotein of lymphocytic choriomeningitis virus, as a fusion with the enhanced green fluorescent protein (RA59-gfp/gp33). P14 splenocytes (transgenic for a T-cell receptor specific for the gp33 epitope) were transferred at different times pre- and postinfection (p.i.). Adoptive transfer of P14 splenocytes 1 day prior to infection with RA59-gfp/gp33, but not control virus lacking the gp33 epitope, RA59-gfp, reduced weight loss and viral replication and spread in the brain and to the spinal cord. Furthermore, demyelination was significantly reduced compared to that in nonrecipients. However, when P14 cells were transferred on day 3 or 5 p.i., no difference in acute or chronic disease was observed compared to that in nonrecipients. Protection in mice receiving P14 splenocytes prior to infection correlated with a robust gp33-specific immune response that was not observed in mice receiving the later transfers. Thus, an early robust CD8$^+$ T-cell response was necessary to reduce virus replication and spread, specifically to the spinal cord, which protected against demyelination in the chronic phase of the disease.

The capacity of the host immune response to control viral replication and spread throughout the central nervous system (CNS) is a critical determinant of mouse hepatitis virus (MHV) pathogenesis. However, the degree to which the immune response, specifically activated virus-specific CD8$^+$ T cells, may contribute to neurological disease during the acute and chronic phases of MHV infection has not been clearly defined. MHV strain A59 induces CNS disease in susceptible mice, providing an animal model to study virus-induced acute encephalitis, as well as primary demyelination.

MHV is a member of the coronavirus family, which contains very large positive-stranded RNA genomes of approximately 30 kb. These viruses infect many vertebrate hosts and induce a variety of diseases ranging in severity. For example, while human coronaviruses 229E and OC43 are responsible for causing the common cold in humans, the recently identified coronavirus severe acute respiratory syndrome is responsible for very severe and potentially lethal respiratory disease (7). The outcome of MHV-induced disease is dependent on several factors, including the age and strain of the mouse, the strain of MHV, and the route of virus inoculation. A59 is a dual-tropic virus infecting both the liver and the CNS. Within the CNS, A59 infects primarily neurons but also glial cells and endothelial cells (14, 25). Following intracranial (i.c.) infection with A59, 4-week-old C57BL/6 (B6) mice develop mild to moderate encephalitis and moderate hepatitis with virus titers peaking between days 3 and 5 postinfection (p.i.) (12). Infectious virus is cleared within the first 10 to 14 days; however, at this time mice begin to develop primary demyelination, either subacute or accompanied by hind limb paralysis (13, 30). At the onset of demyelination, infectious virus is no longer detectable in the CNS but viral RNA can be detected for up to a year p.i. (8).

Virus clearance requires both CD8$^+$ and CD4$^+$ T cells (26, 28, 29). Infections of β2-microglobulin knockout ($\beta_2M^{-/-}$) mice revealed that CD8$^+$ T cells responding to the endogenous H-2K^b epitope within the spike protein S598-605 (S598) are necessary for clearance of A59 as these mice are extremely sensitive to even low doses of virus and experience delayed kinetics of viral clearance (9). CD4$^+$ T cells are necessary for proper CD8$^+$ T-cell activation, survival, and retention in the infected CNS (26, 27). Clearance of infectious virus is mediated by both cytolytic and cytokine-mediated mechanisms; while oligodendrocytes require gamma interferon (IFN-γ), astrocytes and microglia are targeted by perforin and the mechanisms controlling virus replication in neurons are largely unknown but may include noncytolytic mechanisms such as the effects of cytokines and antibody (22).

Demyelination is a complex process, and while the precise mechanisms of this pathology are unclear, on the basis of studies with the highly neurovirulent JHM strain of MHV, MHV-induced demyelination is thought to be primarily immune mediated (10, 33). Demyelination can be completely eliminated in JHM-infected, recombinase-activating gene-deficient ($RAG^{-/-}$) mice that lack functional T and B cells, and this can be reversed upon transfer of splenocytes from immunocompetent mice (35). It has also been shown by depletion and transfer studies in the JHM model that either CD4$^+$ or

* Corresponding author. Mailing address: Department of Microbiology, University of Pennsylvania, School of Medicine, 36th St. and Hamilton Walk, Philadelphia, PA 19104-6076. Phone: (215) 898-8013. Fax: (215) 573-4858. E-mail: weisssr@mail.med.upenn.edu.

$CD8^+$ T cells can induce demyelination (35). On the contrary, A59-induced demyelination has been shown to develop in the absence of B and T cells (18). Furthermore, depletion of $CD4^+$ or $CD8^+$ T cells after the acute stage of the infection does not reduce demyelination (30). Thus, the role of $CD8^+$ T cells in promoting A59-induced demyelination has not been clearly defined, and it appears that the two closely related strains of MHV may induce demyelination via unique mechanisms.

Our hypothesis is that A59-induced neurovirulence is determined by the extent of virus replication and spread of antigen throughout the CNS; thus, we predicted that epitope-specific $CD8^+$ T cells would impede virus growth and lessen disease severity in the acute phase of infection. To test this hypothesis and to better understand whether virus-specific $CD8^+$ T cells are involved in MHV strain A59-induced CNS disease, we have established an adoptive-transfer model. In this model, mice are infected with RA59-gfp/gp33, a recombinant form of A59 that expresses the H-$2D^b$-restricted $CD8^+$ T-cell epitope gp33-41 (referred to as gp33); this epitope is derived from the glycoprotein of lymphocytic choriomeningitis virus (LCMV). As a source of transferred cells, we used the P14 transgenic mouse, which produces $CD8^+$ T cells specific for this epitope (3). Thus, we adoptively transferred splenocytes from P14 mice into B6 recipients 1 day prior to infection with RA59-gfp/gp33 or during the acute phase of infection, on day 3 or 5 p.i., to determine the kinetics of $CD8^+$ T-cell-mediated protection and/or pathogenesis. Overall, we observed less disease and lower virus titers, as well as reduced spread of virus in the CNS of those animals receiving epitope-specific $CD8^+$ T cells 1 day before infection with RA59-gfp/gp33; this correlated with a robust gp33-specific $CD8^+$ T-cell response within the infected brain. We also observed reduced spinal cord demyelination at 4 weeks p.i. in the animals that received the P14 cells 1 day prior to infection. Interestingly, adoptive transfer of P14 splenocytes into acutely infected B6 mice, on either day 3 or 5 p.i., did not cause either an increase or a decrease in viral titers, virus spread, or demyelination compared to those in RA59-gfp/gp33-infected mice that did not receive P14 cells. Thus, we demonstrated that virus spread to the spinal cord white matter occurred very rapidly and protection from demyelination correlated with the recruitment of high numbers of virus-specific $CD8^+$ T cells that inhibited virus spread to the spinal cord during the acute phase of infection.

MATERIALS AND METHODS

Mice and viruses. Four-week-old male mice were used in all experiments; B6 or B6-LY5.2/Cr (CD45.1) mice were obtained from the National Cancer Institute, and $\beta_2M^{-/-}$ mice (B6 background) were obtained from Jackson Laboratories. P14 mice (3) were bred at the University of Pennsylvania. Recombinant MHV strain A59 expressing enhanced green fluorescent protein (EGFP) (referred to here as RA59-gfp) was derived from MHV strain A59 by targeted recombination as previously described (6). Selection of RA59-gfp expressing the LCMV gp33 epitope as a fusion protein with EGFP, referred to as RA59-gfp/gp33, is described elsewhere (5). Briefly, a double-stranded DNA fragment containing the coding region for the first nine complementary synthetic oligonucleotides and 63 amino acids of MHV ORF4a (including the initiation AUG codon), followed by the coding region for the 9 amino acids of gp33, was generated from complementary synthetic oligonucleotides 63 bases in length. This fragment was ligated into pEGFP (Clontech) such that the ORF4a/gp33 fragment was adjacent to and in frame with the gene for EGFP. The fragment containing ORF4a/gp33/EGFP was cleaved from this plasmid with SalI and NotI and inserted into pMH54-EGFP (6) to replace most of gene 4. Targeted recombination of donor RNA transcribed from pMH54-EGFP containing the gp33 sequences and the recipient virus fMHV was carried out with feline FCWF cells (5). Recombinant viruses were selected by two rounds of plaque purification on L2 cells, and sequencing was performed to verify the presence of gp33 (5).

Isolation of mononuclear cells from spleens for adoptive transfer. Spleens were removed from P14 mice. Suspensions were prepared by homogenizing spleens in a nylon bag (mesh opening size of 64 μm) with a syringe plunger in RPMI 1640 medium supplemented with 1% fetal calf serum. Red blood cells were lysed with 0.83% ammonium chloride, and the lymphocyte suspension was washed twice in 1× phosphate-buffered saline (PBS) and resuspended in 1× PBS for transfer.

Intravenous (i.v.) injection and i.c. inoculation of mice. Adoptive transfer of 2×10^7 cells in 0.5 ml of 1× PBS to 4-week-old B6 mice was achieved through i.v. injection via the tail. Mice received P14 cells 1 day prior to infection with A59-gfp/gp33 or A59-gfp. For i.c. infections, mice were anesthetized with isoflurane, and 30 μl containing 10^5 PFU of virus diluted in 1× PBS–0.75% bovine serum albumin was injected into the left cerebrum.

Virus replication in mice. To measure in vivo virus replication, mice were sacrificed on days 3, 5, 7, 10, and 28 p.i. Mice were perfused with 10 ml of 1× PBS, and their brains were removed. The left half of each brain was placed in 3 ml of gel saline (an isotonic saline solution containing 0.167% gelatin), weighed, and stored frozen at −80°C. Brains were subsequently homogenized, and standard plaque assays were performed with L2 mouse fibroblast monolayers (12). The right half of each brain was placed in 10% phosphate-buffered formalin to fix for histology and viral antigen staining.

Histologic and immunohistochemical analyses. The right halves of brains and entire spinal cords from animals sacrificed at days 3, 5, and 7 p.i. were fixed in formalin, embedded in paraffin, sectioned, and stained for viral antigen or inflammation. Antigen staining was performed by the avidin-biotin-immunoperoxidase technique (Vector Laboratories, Burlingame, Calif.) by using diaminobenzidine tetrahydrochloride as the substrate and a 1:20 dilution of rabbit antinucleocapsid monoclonal antibody (kindly provided by Julian Leibowitz). All slides were read in a blinded manner, and groups of at least four mice were examined in two separate experiments for each virus and treatment. Hematoxylin-and-eosin (H-and-E) staining for inflammation was carried out, and analysis was performed in a blinded manner by a neuropathologist. The encephalitis scores used to classify inflammation were as follows: 0, no specific pathological changes within the brain parenchyma; 1, few perivascular cuffs with minimal extension into the parenchyma and some vacuolation and cell loss; 2, same as 1 except more areas affected; 3, neuropil vacuolation and/or cell loss; 4, widespread vacuolation and/or cell loss.

Isolation of mononuclear cells from the brain for analysis. Mononuclear cells from the brain were prepared as previously described (5, 24) on days 7, 10, 12, and 28 p.i. Cells harvested from five or six brains per group were pooled. Cells were passed through a 30% Percoll gradient and then passed through a cell strainer (70-μm pore diameter; Becton Dickinson). The cell suspension was layered atop a 2-ml Lymphocyte-M (Cedarlane Laboratories) cushion, and viable cells were removed from the interface, washed with 1× PBS, and counted.

Intracellular IFN-γ staining and flow cytometry analysis. Intracellular IFN-γ secretion was assayed in response to stimulation with specific peptides as previously described (19, 25). Brain-derived mononuclear cells or splenocytes (10^6) were cultured with 10 U of human recombinant interleukin-2–1 μl of brefeldin A (Golgiplug; PharMingen) per ml either with or without 1 μg of specific peptide per ml in a total volume of 200 μl of RPMI 1640 medium supplemented with 5% fetal calf serum for 5 h at 37°C. Cells were then stained for surface expression of CD8, CD4, and/or CD45.2 with monoclonal antibodies specific for CD8a (clone 53-6.7), CD4 (clone RM4-5), and CD45.2 (clone 104) (PharMingen). After surface staining, intracellular IFN-γ was detected by first fixing and then permeabilizing cells with the Cytofix/Cytoperm kit (PharMingen) and stained with a fluorescein isothiocyanate-conjugated monoclonal rat anti-mouse IFN-γ antibody (clone XMG 1.2; PharMingen). Cells were analyzed with a FACScan flow cytometer (Becton Dickinson). The total number of cells positive for IFN-γ per mouse was determined by multiplying the fraction of cells positive for IFN-γ by the total number of live cells isolated per brain.

Demyelination. Demyelination was analyzed for both quantity and severity. Analysis of demyelination was performed on spinal cords harvested from animals 28 days p.i. Five to eight mice were examined in each of two separate experiments. After sacrifice, mice were perfused with 10 ml of 1× PBS and their spinal cords were removed. Spinal cords were sectioned into five regions representing the cervical through lumbar regions and embedded in paraffin for sectioning. Cross sections were stained with a myelin-specific dye, luxol fast blue. To determine the percentage of demyelinated spinal cord, quadrants of spinal cord were counted. At least 10 sections of cord were counted for each animal. A description

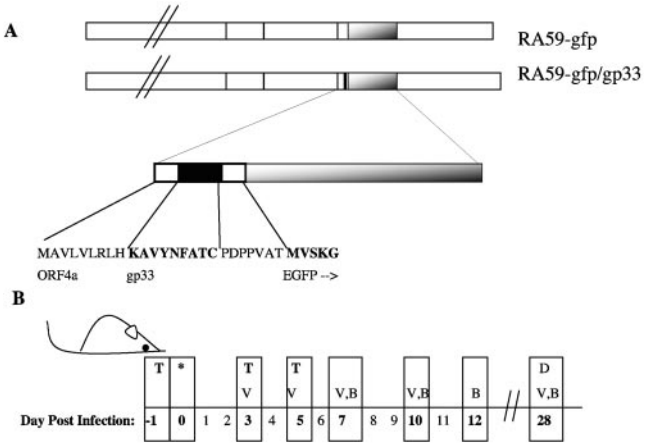

FIG. 1. Experimental design. (A) Schematic of viruses selected by targeted recombination. Targeted recombination of synthetic RNAs transcribed from pMH54 that contained the coding sequence for the gp33 epitope, followed by the gene for EGFP in place of ORF4a, was carried out as described in the text. The region encoding the introduced sequences is shown, as are the genomes of the two viruses that were selected, one containing the gp33 epitope fused to the gene for EGFP and the other containing just the gene for EGFP (5, 6). (B) Schematic of the adoptive transfer of P14 cells and infection with the RA59-gfp/gp33 and RA5-gfp. Infection was performed on day 0 (*), and transfers (indicated by the letter T) were performed on day 3 or 5 p.i. or on the day prior to infection. Virus titers (V) were determined on days 3, 5, 7, 10, and 28 p.i.; brain lymphocytes (B) were isolated for analysis on days 7, 10,12, and 28 p.i.; and demyelination (D) was scored on day 28 p.i.

of the pathology score used to analyze the severity of demyelination is as follows: 0, no demyelination; 1, small foci of demyelination seen in less than 1 section per slide (containing a total of 10 sections of cord); 2, one to three small areas of demyelination per slide; 3, at least one large region of demyelination per slide and all sections containing some demyelination; 4, ample demyelination involving all sections with one to three large areas of demyelination; 5, all sections involved with more than three large regions of demyelination, confluent and involving the medulla oblongata.

RESULTS

Reduced weight loss in early transfer recipients infected with RA59-gfp/gp33. In order to assess the role of epitope-specific $CD8^+$ T cells during the acute phase of infection with A59, we developed an adoptive-transfer system with splenocytes from P14 mice, which produce gp33-specific CD8 T cells (3), and a recombinant form of strain A59 that expresses the gp33 epitope as a fusion protein with EGFP (RA59-gfp/gp33). Figure 1A shows schematic diagrams of the genomes of RA59-gfp/gp33 and control virus RA59-gfp (5). Nonessential gene 4 was replaced with a small piece of ORF4a and the gfp/gp33 fusion. Elimination of expression of ORF4 has previously been shown to have no effect on virulence of MHV in the CNS (21). As shown in Fig. 1B, in the adoptive-transfer model, 4-week-old B6 mice received 2×10^7 P14 splenocytes i.v. 1 day prior to i.c. infection or on day 3 or 5 p.i. with 10^5 PFU of either RA59-gfp/gp33 or control virus RA59-gfp, which does not express the gp33 epitope. Control animals that did not receive an adoptive transfer were also infected with either RA59-gfp/gp33 or RA59-gfp. To assess clinical symptoms, mice were weighed prior to infection and on various days p.i. Compared to mock-infected animals, mice infected with RA59-gfp/gp33 lost significant weight by day 7 p.i. (Fig. 2A). Animals that received gp33-specific $CD8^+$ T cells prior to infection with the gp33-expresssing virus lost significantly less weight by day 7 p.i. ($P < 0.001$) than did mice receiving a transfer on day 3 or 5 p.i. and those animals not receiving a transfer (Fig. 2A). RA59-gfp-infected mice lost similar amounts of weight with or without a transfer of P14 cells (Fig. 2B). Thus, adoptive transfer of epitope-specific cells prior to, but not during, infection with

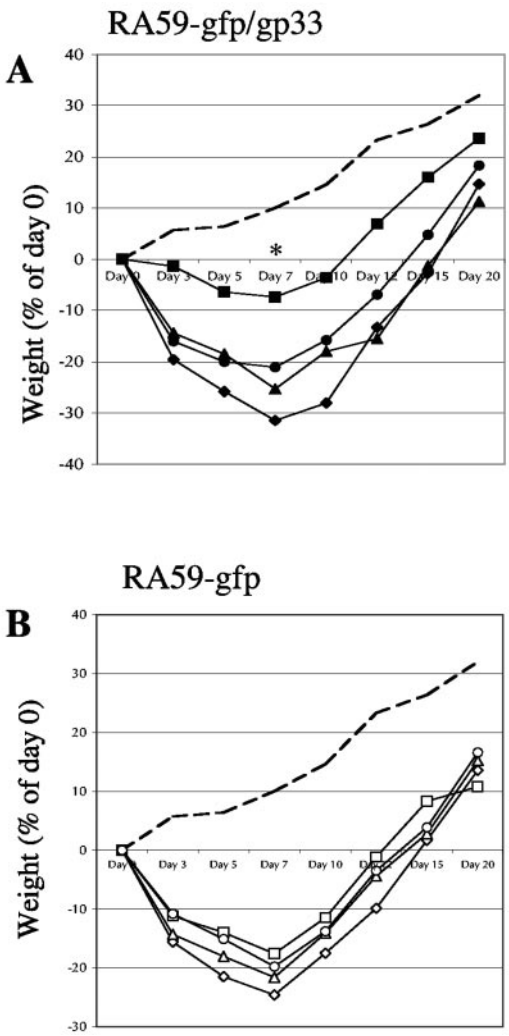

FIG. 2. Weight loss is reduced in mice that received adoptive transfer of epitope-specific $CD8^+$ T cells prior to infection with RA59-gfp/gp33. Four-week-old B6 mice received 2×10^7 P14 cells in PBS via tail vein injection 1 day prior to infection (squares) or on day 3 (triangles) or 5 (circles) p.i. with 10^5 PFU of RA59-gfp/gp33 (A) or RA59-gfp (B). A corresponding group did not receive the adoptive transfer prior to infection (diamonds). Mice were weighed on days 0, 3, 5, 7, 12, 15, and 20 days p.i., and the percent weight change compared to the starting weight was calculated. The percent weight change of mock-infected controls (dashed line, $n = 5$) steadily increased over the course of time analyzed. RA59-gfp/gp33-infected mice receiving P14 splenocytes prior to infection experienced significantly less weight loss on day 7 p.i. compared to the other groups ($P < 0.001$, two-sided t test) (A). Animals infected with RA59-gfp lost significant weight compared to controls, but there were no differences observed due to P14 splenocyte transfer (B).

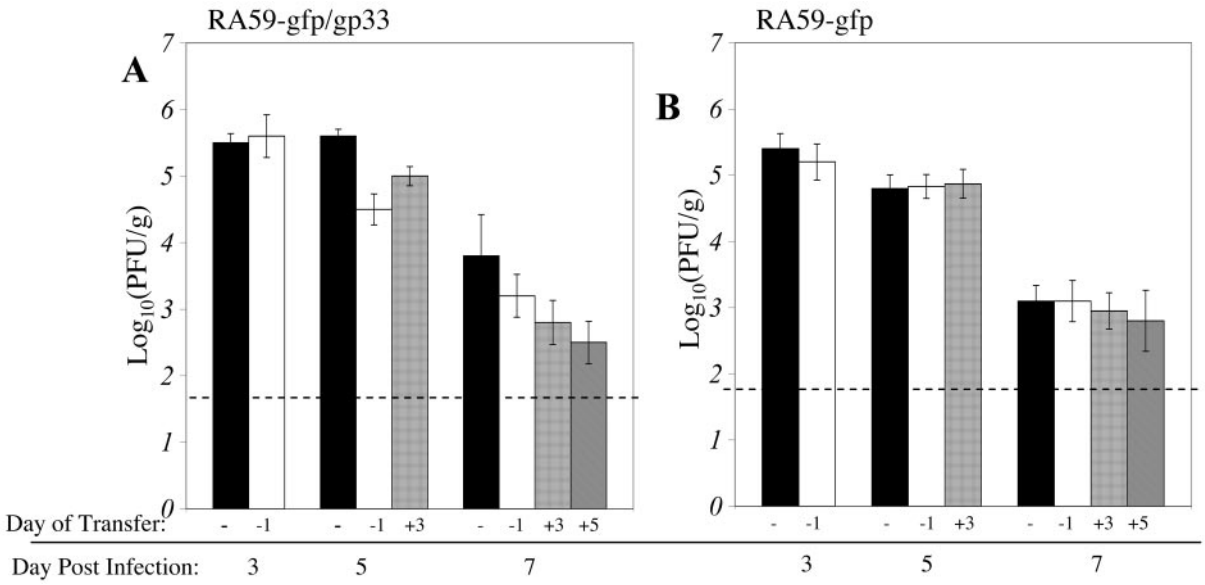

FIG. 3. Virus replication in brains after infection and transfer of gp33-specific CD8+ T cells. One day prior to infection or on day 3 or 5 p.i. with 10^5 PFU of either RA59-gfp/gp33 or RA59-gfp, mice received i.v. transfer of 2×10^7 P14 splenocytes, as shown below each bar. Represented are the titers determined from brains harvested on days 3, 5, and 7 p.i. (A) On day 5 p.i., mice infected with RA59-gfp/gp33 and having received the adoptive transfer of P14 cells prior to infection (open bar) had significantly reduced virus titers compared to those of animals infected with RA59-gfp/gp33 that did not (closed bar) (two sided *t* test, $P < 0.001$) and those that received the transfer on day 3 p.i. ($P < 0.05$). There were no significant differences between groups on day 7 p.i. (B) There were no differences in virus titers between RA59-gfp-infected animals not receiving the transfer (closed bar) and animals that received the transfer 1 day before infection (open bar), on day 3 p.i. (checked bar), or on day 5 p.i. (striped bar). The data represent the averages and standard error bars from five to seven animals per group per day from one representative experiment (of two). The limit of detection is indicated by the dashed line.

MHV protected against the severe weight loss associated with the acute phase of infection.

Virus titers, antigen spread, and encephalitis in the brain after transfer of epitope-specific CD8+ T cells. First, we measured the effect of the transferred epitope-specific CD8+ T cells on viral titers in the brains of infected mice. Compared to mice that did not receive P14 cells, those that received the transfer prior to infection had a significant ($P < 0.001$) reduction in virus titers of approximately 20-fold on day 5 p.i. (Fig. 3A). In addition, animals that received the P14 cell transfer on day 3 p.i. had titers similar to those of the nonrecipients and their titers were significantly greater than those of the animals that received the transfer prior to infection ($P < 0.05$). However, on day 7 p.i., the titers in all groups were low and no significant differences were observed (Fig. 3A). Control mice infected with RA59-gfp that received gp33-specific CD8+ T cells exhibited no difference in titers compared to those of nonrecipients, as expected, demonstrating that the CD8+ T-cell response is specific. Thus, the transfer of naive, epitope-specific CD8+ T cells was capable of protecting against virus replication when the transfer was done i.v. prior to infection. In all RA59-gfp/gp33- and RA59-gfp-infected animals, with or without having received the P14 cells, titers were undetectable on days 10 and 28 p.i. (data not shown).

We have previously observed that spread of viral antigen in the brain, compared with viral titers, is a more accurate indication of the severity of CNS damage (25, 31). In order to assess virus spread, we examined viral antigen in sagittal sections of brains that were harvested at different times p.i. with a monoclonal antibody directed at the viral nucleocapsid protein. The peak of virus antigen expression was on day 5 p.i. in the brain; virus antigen staining was very low on day 3 p.i., despite high titers, and was almost undetectable on day 7 in all of the sections examined from each group (data not shown). Several regions of the brain that were consistently involved during the infection included the basal ganglia, the olfactory bulb, the subiculum, the hypothalamus, and the hindbrain, including the medulla and pons. Correlating with the difference in titers observed on day 5, dramatically less antigen staining was observed throughout the brain, as represented in the subiculum and hindbrain, in mice that received gp33-specific CD8+ T cells prior to infection (Fig. 4B and E). Only small foci of antigen-positive cells existed in examined sections from animals that received the transfer prior to infection. However, animals that received the transfer on day 3 p.i. had an amount of viral antigen similar to that in mice that did not receive a transfer, as shown in the subiculum and the hindbrain (Fig. 4). As expected, control animals infected with RA59-gfp had similar levels of antigen with or without having received the transfer (data not shown).

Encephalitis was determined by H-and-E staining of sagittal brain sections and spinal cord cross sections taken on day 7 p.i., the typical peak of inflammation. In agreement with observations of reduced weight loss in RA59-gfp/gp33-infected mice that received the adoptive transfer prior to infection (Fig. 2A), we observed a significant reduction in inflammation (Table 1). H-and-E-stained sections from mice that received the transfer prior to infection revealed a reduction in infiltrating inflammatory cells, little to no pathological changes within the pa-

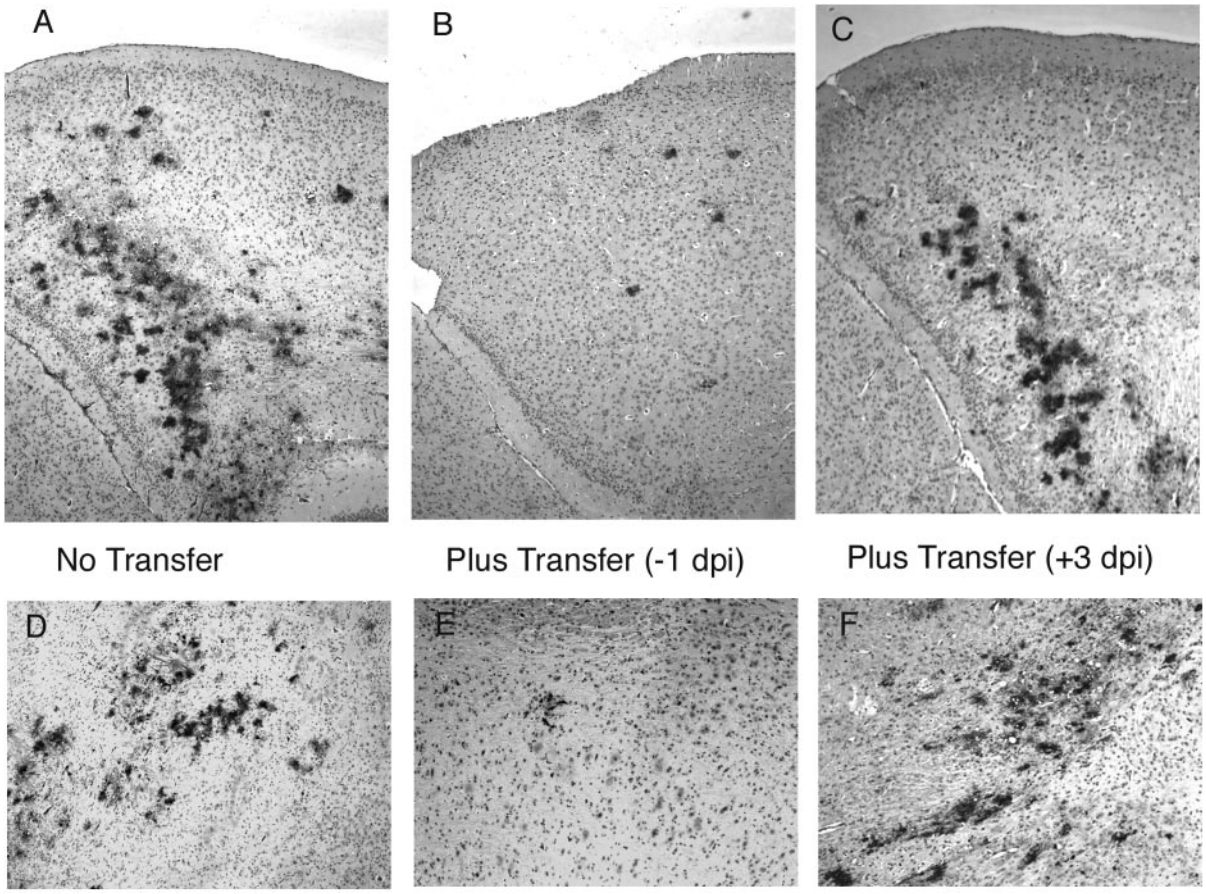

FIG. 4. Antigen spread in brains of RA59-gfp/gp33-infected mice receiving virus-specific $CD8^+$ T cells. Brain samples from mice were preserved in formalin, embedded in paraffin, and sectioned sagittally. Sections were stained by an avidin-biotin immunoperoxidase method with a monoclonal antibody directed against the nucleocapsid protein. Representative sections from day 5 p.i., which was the peak of viral antigen detection, are shown; sections represent samples from two separate experiments with at least five animals per group. Brain sections from mice that did not receive the transfer show intense antigen staining in the subiculum and the medulla, two regions of the brain consistently positive for antigen at this time point (A and D). Transfer recipients (day −1 p.i.), however, have little viral antigen in both of these regions (B and E). Mice that received the transfer at 3 days p.i. (dpi) demonstrated levels of antigen staining similar those of the mice that did not receive the transfer (C and F). Magnification, ×80.

renchyma, and minimal perivascular cuffing compared to all other groups of infected mice (Table 1).

Early transfer of epitope-specific $CD8^+$ T cells blocks virus spread to the spinal cord. Previous studies with the JHM strain of MHV demonstrated that the virus spreads from the brain into the spinal cord between days 7 and 10 p.i. (23). However, virus spread from the brain to the spinal cord during the acute phase of infection with the A59 strain of MHV has not been examined. Thus, we examined spinal cords harvested from infected mice at days 5 and 7 p.i. to determine the kinetics of viral antigen spread. Immunohistochemical analysis with the antinucleocapsid antibody was performed on cross sections of formalin-fixed spinal cord. Robust viral antigen expression was detected on day 5 p.i. in RA59-gfp/gp33-infected animals that did not receive the adoptive transfer (Fig. 5A and B) or received the day 3 p.i. adoptive transfer (Fig. 5E and F), but no antigen was detected in animals that received the transfer prior to infection (Fig. 5C and D). On day 7 p.i., viral antigen was still detectable in all of the animals except those that received the transfer prior to infection (data not shown). Virus antigen

TABLE 1. Encephalitis scores

Transfer[a]	Encephalitis score[b]	
	RA59-gfp/gp33	RA59-gfp
None	2.75 ± 0.71	2.60 ± 0.52
−1 dpi	0.71 ± 0.49[c]	2.4 ± 0.55
+3 dpi	2.5 ± 1.2	2.2 ± 0.45
+5 dpi	2.38 ± 1.1	2.24 ± 0.97

[a] Adoptive transfer of P14 splenocytes was performed on the days indicated prior to or after infection with RA59-gfp/gp33 or RA59-gfp as described in the text and Materials and Methods. dpi, day(s) p.i.

[b] Sagittal sections of formalin-fixed brain samples were stained with H and E and scored by a neuropathologist. The range of scores was 0 to 4, with 4 representing the most severe inflammation (see Materials and Methods). The score for each group represents an average and standard deviation pooled from four or five mice from at least two separate experiments with two sections per slide.

[c] RA59-gfp/gp33-infected mice that received the adoptive transfer prior to infection had significantly reduced encephalitis scores than the no-transfer group ($P < 0.001$) or the group receiving a transfer on day 3 or 5 p.i. ($P < 0.003$) (two-sided t test). There were no significant differences among the groups of RA59-gfp-infected animals.

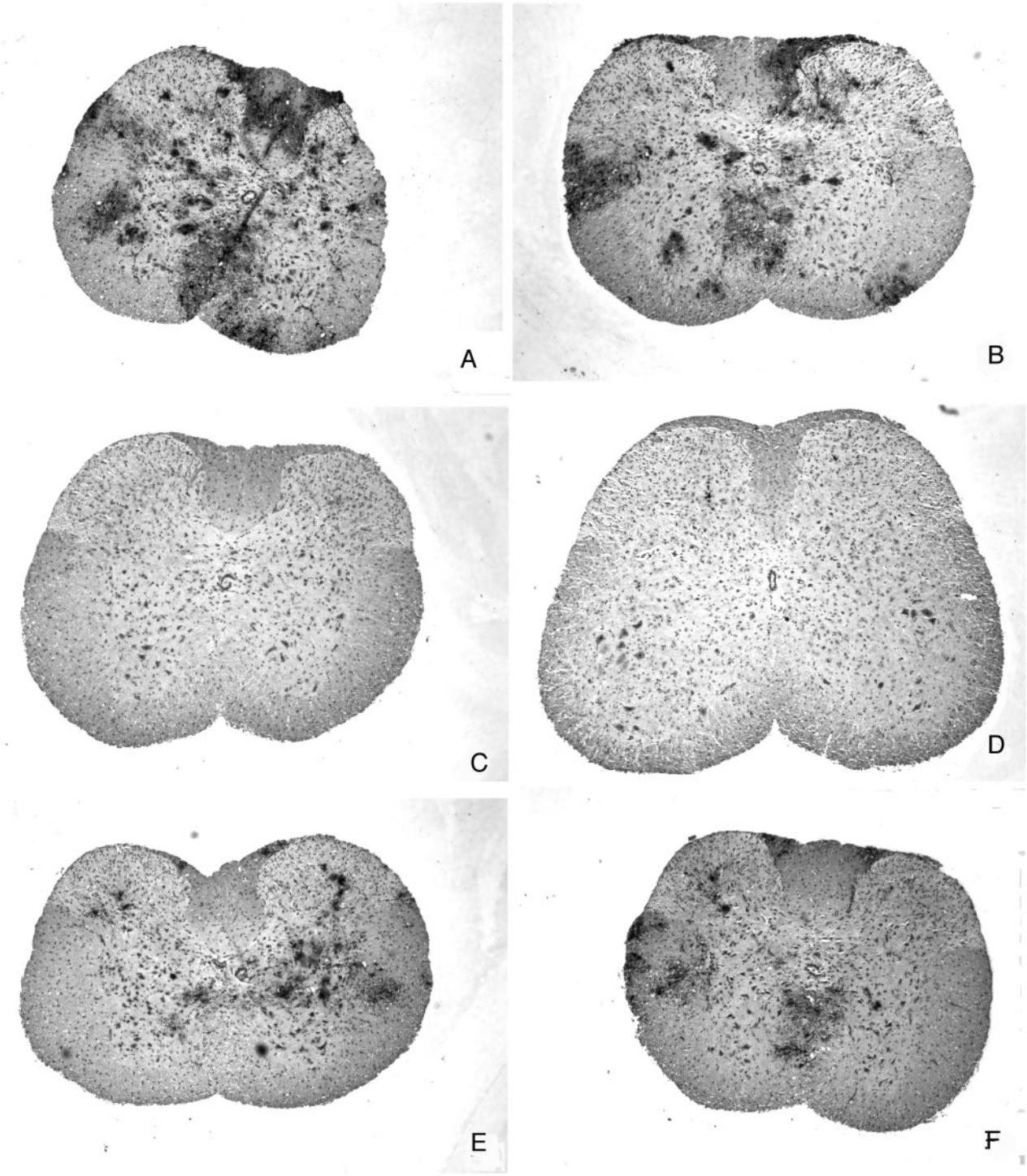

FIG. 5. Early transfer of P14 splenocytes blocks spread of virus to the spinal cord in RA59-gfp/gp33-infected animals. Spinal cords were harvested from infected mice on day 5 p.i., fixed in formalin, and embedded in paraffin, and cross sections were stained for viral antigen as described in the legend to Fig. 4 and Materials and Methods. On day 5 p.i., staining revealed antigen in nearly every section from all RA59-gfp/gp33-infected animals (A and B) but not in the day −1 transfer recipients (C and D). On day 5 p.i. the day 3 transfer recipients had levels of antigen in spinal cords similar to those of animals that did not receive the adoptive transfer (E and F). On day 5 p.i., antigen is clearly detected in the gray and white matter in the non-transfer recipients and the animals that received the transfer on day 3 p.i. Magnification, ×32.

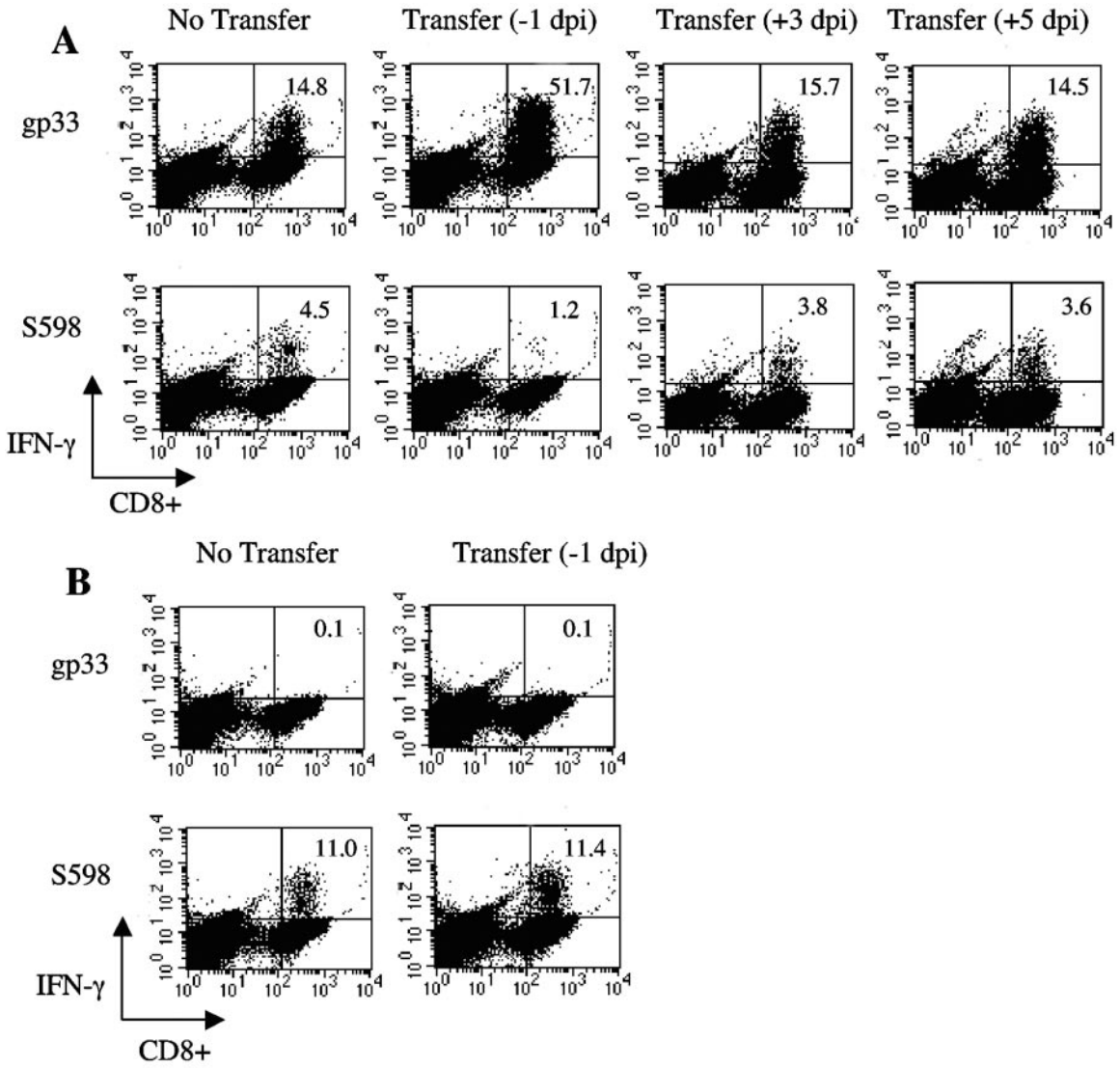

FIG. 6. IFN-γ-secreting, MHV-specific $CD8^+$ T cells after i.c. infection. Localized effector $CD8^+$ T cells were harvested from brains at 7 days p.i. (dpi) with RA59-gfp/gp33 or RA59-gfp with or without having received P14 cells on various days. $CD8^+$ T cells were examined for IFN-γ secretion in response to gp33 (top row) or S598 (bottom row) peptide. (A) On day 7 p.i., cells derived from RA59-gfp/gp33-infected animals exhibited a strong gp33-specific response; animals that received the transfer prior to infection had an increased gp33-specific $CD8^+$ T-cell response that corresponded to a reduced response to the S598 epitope. (B) RA59-gfp-infected animals did not contain brain-derived activated gp33-specific $CD8^+$ T cells but had a strong response to S598, as expected and previously reported (5). The data shown represent cells pooled from the brains of four to six animals for each group and are representative of two independent experiments. In all panels, the percentage in the upper right quadrant is the percentage of the total number of $CD8^+$ T cells that were epitope-specific IFN-γ-secreting cells.

was detected in both the gray and white matter on day 5 p.i. (Fig. 5), whereas on day 7 p.i. virus antigen was only detected in the white matter (data not shown). Thus, corresponding to the detection of virus antigen in the brain, virus spread to the spinal cord is reduced only when gp33-specific $CD8^+$ cells are transferred prior to infection.

Early recruitment and activation of gp33-specific $CD8^+$ T cells correlates with reduced CNS disease. To evaluate the degree to which the recombinant virus could elicit an immune response to the introduced gp33 epitope and thus how well the transferred cells engrafted, we sought to determine the activation status of virus-specific $CD8^+$ T cells in animals that had or had not received the transfer of P14 cells. In order to accurately assess the role of the transferred epitope-specific $CD8^+$ T cells at the site of infection, we obtained mononuclear cells from the brains of infected mice on day 7 p.i., the typical peak of lymphocyte infiltration in the brain after i.c. infection with A59. More than half (51.7%) of the $CD8^+$ T cells harvested from the brains of RA59-gfp/gp33-infected mice that received the adoptive transfer of gp33-specific $CD8^+$ T cells were specific for gp33 on day 7 p.i. (Fig. 6A). In contrast, only 14.8% of the brain-derived $CD8^+$ T cells were activated and specific for the gp33 epitope in mice that did not receive the adoptive transfer; this reflected the normal primary immune response and is similar to previously reported results (5). Interestingly, mice that received the adoptive transfer on either day 3 or 5 p.i.

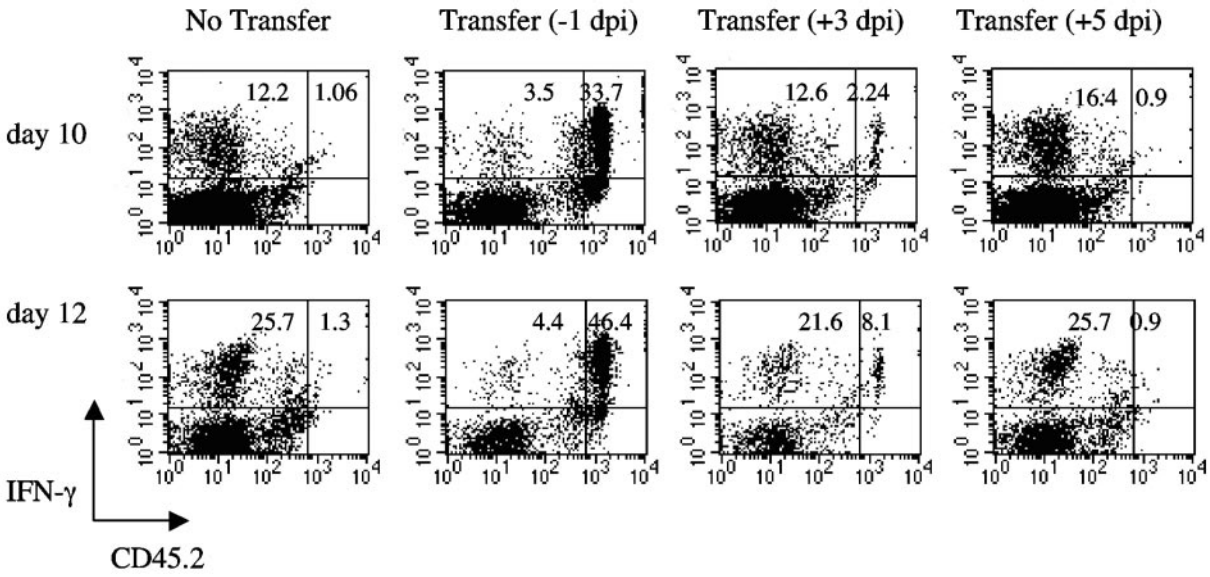

FIG. 7. Brain infiltration and activation of adoptively transferred gp33-specific CD8+ T cells during infection with RA59-gfp/gp33. At 10 and 12 days p.i. (dpi), cells were harvested from B6/LY-5.1 mice infected with RA59-gfp/gp33 having received either no transfer or a transfer of P14 cells 1 day prior to infection or on day 3 or 5 p.i. Cells were prepared and assayed for IFN-γ secretion as described in the legend to Fig. 6. A robust gp33-specific CD8+ T-cell response was observed for all infected animals, but CD45.2-positive cells were only detected in the brains of animals that received the transfer prior to infection or on day 3 p.i. The total percentage of gp33-specific CD8+ T cells was greater on day 12 (bottom row), reflecting the diminished number of CD8+ T cells at this time point compared to that on day 10 p.i. (top row). Represented is the total number of CD8+ T cells. The percentage in the upper left quadrant represents the endogenous gp33-specific CD8+ T-cell response (CD45.2 negative), whereas the percentage in the upper right quadrant represents the transferred P14 cells (CD45.2 positive).

had percentages of gp33-specific CD8+ T cells similar to those of animals that did not receive the transfer (15.7 and 14.5%, respectively).

In order to understand how the response to an immunodominant epitope may affect the response to other, less dominant epitopes, we analyzed the response to the endogenous epitope in the spike protein S598. Animals infected with RA59-gfp, lacking the gp33 epitope, contained a higher percentage of

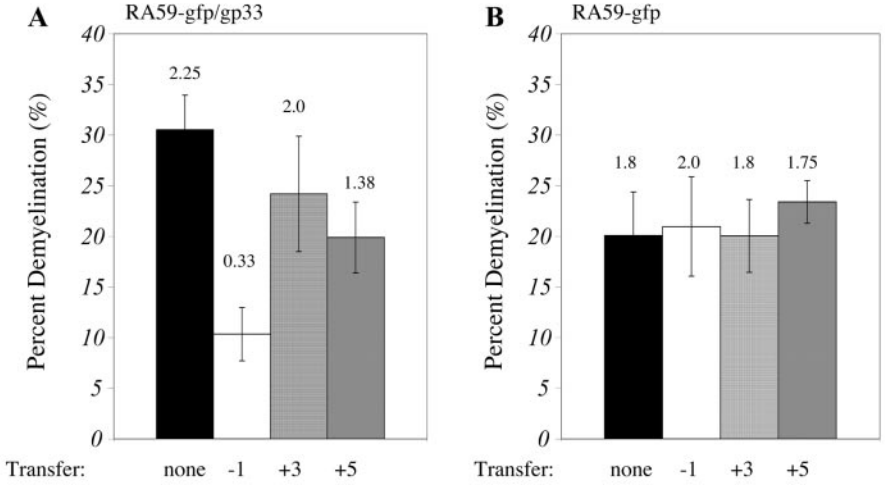

FIG. 8. Demyelination is reduced in animals protected from acute disease. The percentage and severity of demyelination were examined on day 28 p.i. Spinal cords were removed from mice 4 weeks p.i., and cross sections of formalin-fixed, paraffin-embedded spinal cord were stained with luxol fast blue. Percent demyelination reflects the number of demyelination-containing quadrants; at least 20 quadrants were counted for each mouse, and the data from five to eight mice examined for each group in each of two separate experiments were pooled. The value above each bar is the pathology score (described in Materials and Methods). Error bars represent the standard error of the mean. (A) Mice infected with RA59-gfp/gp33 that received P14 cells (open bar) had significantly less severe demyelination than did similarly infected mice that did not receive P14 cells (closed bar) or received cells on day 3 p.i. ($P < 0.001$) or mice that received cells on day 5 p.i. ($P < 0.01$, two-sided t test). (B) Animals infected with RA59-gfp with or without transfer of P14 cells had similar percentages of demyelination that produced similar severity scores.

$CD8^+$ T cells specific for the endogenous S598 epitope than did the RA59-gfp/gp33-infected animals (Fig. 6B). RA59-gfp/gp33-infected mice that received the transfer prior to infection exhibited the lowest percentage of S598-specific $CD8^+$ T cells (1.2%), perhaps because of the very high number of activated gp33-specific $CD8^+$ T cells (Fig. 6A).

In order to determine if the lower numbers of gp33-specific $CD8^+$ T cells observed in the mice that received the adoptive transfer on day 3 or 5 p.i., compared to the group that received the transfer prior to infection, was due to the kinetics of activation and recruitment into the brain, we analyzed brain-derived mononuclear cells for gp33-specific $CD8^+$ T cells on days 10 and 12 p.i. (which corresponds to day 7 posttransfer for each transfer recipient group). To distinguish between the transferred P14 cells and the endogenous gp33-specific $CD8^+$ T cells, we used B6-LY5.2/Cr mice (CD45.1) as recipients; thus, the CD45.2-positive cells reflect the adoptively transferred P14 cells. We observed an overall increase in the percentage of gp33-specific $CD8^+$ T cells on day 12 (Fig. 7, bottom row) compared to day 10 (Fig. 7, top row), and this reflects a decrease in the total number of $CD8^+$ T cells in the brain and retention of virus-specific $CD8^+$ T cells. As expected, no CD45.2 cells were detected in animals that did not receive the adoptive transfer (Fig. 7). The majority of the IFN-γ-secreting, gp33-specific $CD8^+$ T cells were P14 in origin ($CD45.2^+$) in the mice that received the transfer prior to infection. Interestingly, a significantly smaller percentage of the gp33-$CD45.2^+$ gp33-gp33-specific $CD8^+$ T cells were observed in the mice that received the adoptive transfer on day 3 p.i. than in the mice that received the transfer prior to infection (2.24% compared with 33.7%). Furthermore, P14-derived gp33-specific $CD8^+$ cells were completely undetectable on both days 10 and 12 p.i. in mice that received the adoptive transfer on day 5 p.i. Thus, activation and trafficking of naive, virus-specific $CD8^+$ T cells appeared to be limited to the first 3 days of the infection.

Demyelination is reduced in animals protected from acute disease. A focus of this study was to understand how a strong $CD8^+$ T-cell response could shape the outcome of the chronic disease induced by A59. Earlier depletion studies indicated that when $CD8^+$ T cells were depleted after resolution of acute A59 infection, demyelination was nearly the same as in nondepleted mice, which suggested the possibility that $CD8^+$ T cells could initiate disease during the acute phase of infection (30). Mice infected with RA59-gfp/gp33 or RA59-gfp received transfers the day prior to infection or on either day 3 or day 5 p.i. and were sacrificed 4 weeks p.i., at which time their spinal cords were removed, fixed, and stained with a myelin-specific dye, luxol fast blue. Demyelination was assayed by counting quadrants of cross-sectioned spinal cord. We also used a pathology score to describe the severity of demyelination of the spinal cord; the scores ranged from 0, no demyelination evident, to 5, pathology involving severe, confluent demyelination of nearly the entire spinal cord (see Materials and Methods) (Fig. 8).

Mice protected from acute disease via adoptive transfer of gp33-specific $CD8^+$ T cells 1 day prior to infection had significantly less demyelination, as measured by both the percentage of quadrants containing demyelination and the severity of demyelination, than did those that were not protected from acute disease (non-transfer recipients and day 3 and 5 p.i. transfer recipients) (Fig. 8A). The levels of demyelination observed in animals infected with RA59-gfp did not differ, regardless of the adoptive transfer of P14 cells, as expected (Fig. 8B). Thus, protection from demyelination correlated with reduced acute disease, including reduced virus spread.

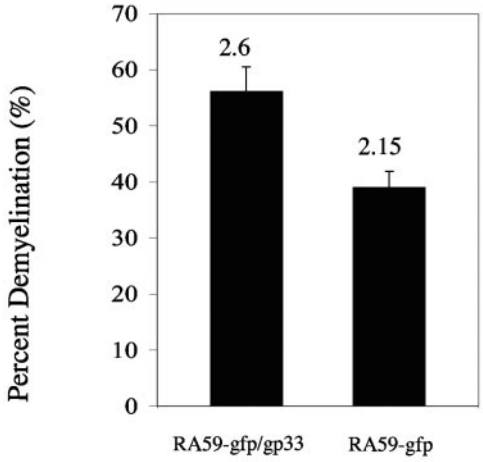

FIG. 9. Demyelination in $\beta_2M^{-/-}$ mice. $\beta_2M^{-/-}$ mice were infected with 250 PFU of either RA59-gfp/gp33 or RA59/gfp. At 4 weeks p.i., mice were sacrificed and spinal cords were removed and prepared for histological and demyelination analyses as described in the legend to Fig. 8. Percent demyelination represents the number of quadrants, in the total number of spinal cord quadrants counted, that were positive for demyelination, and the value above each bar represents the severity score (described in Materials and Methods). RA59-gfp/gp33-infected animals had significantly more demyelinated spinal cord at 4 weeks p.i. than did RA59-gfp-infected animals ($P < 0.001$, two-sided t test). The data shown represent pooled data from at least 20 quadrants per mouse and 10 mice per virus.

We observed that the percentage of demyelinated spinal cord and the severity of spinal cord demyelination were greater in the RA59-gfp/gp33-infected mice than in RA59-gfp-infected animals. We reasoned that this could be due to either a small difference in the kinetics of virus replication and spread or possibly to a pathogenic immune response elicited by the gp33-expressing virus. Infections of $\beta_2M^{-/-}$ mice were carried out to determine whether a detrimental major histocompatibility complex class I-restricted immune response was elicited in RA59-gfp/gp33-infected mice. $\beta_2M^{-/-}$ mice were infected with 250 PFU of either RA59-gfp/gp33 or RA59-gfp, as these mice are highly susceptible to MHV infection. Surprisingly, despite the absence of detectable differences in either virus titers in the brain or virus antigen detection in the brain during the first week of infection (data not shown), RA59-gfp/gp33 still induced significantly more demyelination than did RA59-gfp (Fig. 9). This suggests that demyelination induced by RA59-gfp/gp33 may be more severe because of an intrinsic property of the virus other than immune recognition of the gp33 epitope expressed by RA59-gfp/gp33; however, we cannot completely rule out the possibility that $CD8^+$ T cells can contribute to demyelination in these mice, as they do exist in low numbers.

Retention of epitope-specific $CD8^+$ T cells within the brain after CNS infection. $CD8^+$ T cells have been shown to persist in an activated, IFN-γ-secreting state within the brains of mice

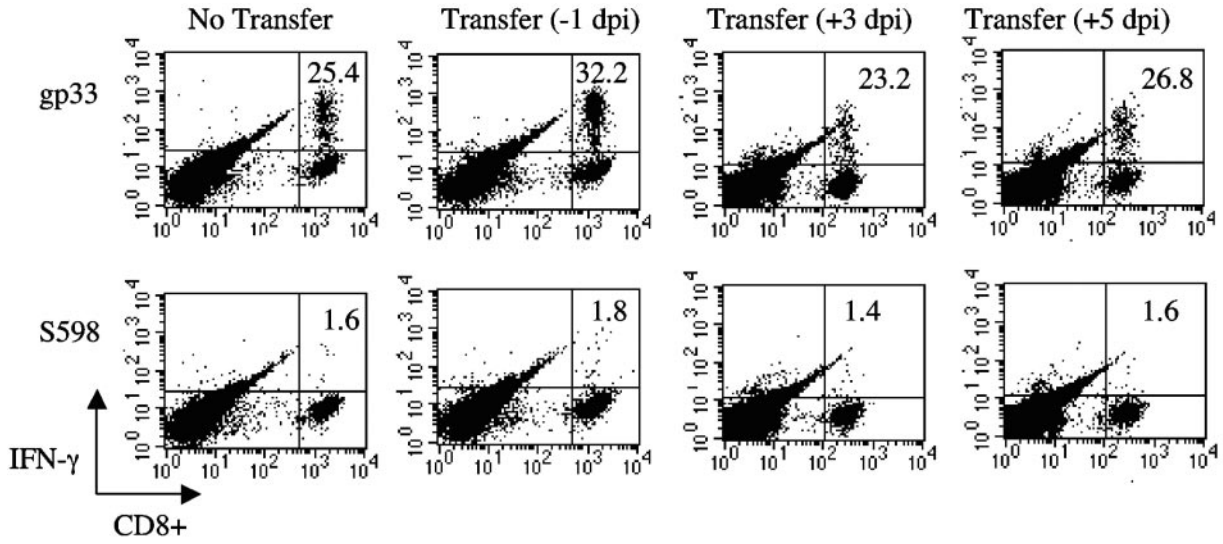

FIG. 10. Retention of gp33-specific CD8+ T cells within the brain after CNS infection with RA59-gfp/gp33. Lymphocytes harvested from brains at 4 weeks p.i. with RA59-gpf/gp33 revealed that a significant percentage of IFN-γ-secreting CD8+ T cells were specific for gp33. Cells were harvested as described in the legend to Fig. 3, and the data shown represent cells pooled from seven animals; in all plots, the percentage in the upper right quadrant is the percentage of IFN-γ-secreting CD8+ T cells that are epitope specific (gp33 specific [top row] or S598 specific [bottom row]). dpi, days postinfection.

after infection with MHV (15), and it has been shown that this is dependent upon the persistence of viral RNA (16). To more clearly understand how the acute phase of infection, as shaped by the transfer of P14 cells, affected the retention of CD8+ T cells during the chronic phase of infection and to determine if retained epitope-specific CD8+ T cells correlated with demyelination, brains were removed 4 weeks p.i. for isolation and analysis of localized inflammatory cells. Brain-derived cells were analyzed for intracellular IFN-γ secretion in response to in vitro peptide stimulation. The total numbers of CD8+ T cells in the brains of all of the animals were similar, although the total number of virus-specific, IFN-γ-secreting CD8+ T cells was about 10-fold higher in RA59-gfp/gp33-infected animals than in RA59-gfp-infected animals, likely because of the response to the immunodominant gp33 epitope in the former (data not shown). In RA59-gfp/gp33-infected animals, the levels of activated gp33-specific IFN-γ-secreting CD8+ T cells were similar but highest in the mice that received the transfer prior to infection (Fig. 10). Thus, we observed that a similar, high number of gp33-specific, IFN-γ-secreting CD8+ T cells was retained in all groups. The percentage of gp33-specific CD8+ T cells did not appear to correlate with the gp33-specific CD8+ T-cell response observed during the acute phase of infection (on day 7, 10, or 12 p.i.; Fig. 6 and 7). A clear correlation between the presence of activated gp33-specific CD8+ T cells and demyelination could not be made; however, it was noted that the day −1 transfer recipients had the lowest levels of demyelination and the highest percentage of gp33-specific CD8+ T cells, whereas the lowest percentage of gp33-specific CD8+ T cells was observed in animals that demonstrated high levels of severe demyelination (no-transfer group and day 3 and 5 p.i. transfer groups; Fig. 8 and 10).

DISCUSSION

Infection with the A59 strain of MHV provides a model for both viral encephalitis and demyelination, but despite extensive study, the mechanism of A59-induced demyelination is still not fully understood. The findings presented here have highlighted several factors that are important in understanding the pathogenesis of A59-induced demyelination, including the relationship between virus spread during the acute phase of infection and its outcome in terms of demyelination, as well as how the kinetics of CD8+ T-cell activation and recruitment to the brain affect virus spread within the CNS.

We have previously examined the role of CD8+ T-cell-mediated protection from A59 infection by a vaccination strategy (5); however, the adoptive-transfer system with splenocytes derived from the P14 mouse has allowed us to go a step further and determine the effects of T cells, specific for one epitope, on pathogenesis. It has also allowed the kinetic analysis of activation and recruitment of naive CD8+ T cells to the infected CNS. In this study we assessed protection from CNS disease achieved by adoptive transfer of naive gp33-specific splenocytes into mice prior to or during the acute phase of infection with a gp33-expressing recombinant form of strain A59. Epitope-specific CD8+ T cells inhibited virus growth and viral antigen spread in the brain and reduced disease severity and inflammation only when transferred prior to infection. This correlated with an increased activated gp33-specific CD8+ T-cell response in the brain. In animals protected from acute disease, there was a dramatic reduction in the level and severity of demyelination at 1 month p.i. This is in agreement with other studies of JHM infection that demonstrated virus spread within the CNS as a major determinant in the development of chronic demyelination (15). Similarly, studies using the trans-

fer of nucleoprotein-specific cytotoxic T lymphocytes was effective at reducing JHM replication within the CNS (28).

Priming of virus-specific $CD8^+$ T cells has been shown to occur very rapidly after infection with a variety of pathogens, and here we show that the window of naive $CD8^+$ T-cell priming, in the context of a virus infection within the CNS, is limited to the first 3 days of infection. Wong and Pamer recently demonstrated a feedback mechanism during infection with *Listeria monocytogenes* by which antigen-presenting cells are eliminated by effector cytotoxic T lymphocytes, thereby limiting the $CD8^+$ T-cell response (34). It is possible that this accounts for the absence of CD45.2-positive, gp33-specific $CD8^+$ T cells observed in the brains of RA59-gfp/gp33-infected mice that had received an adoptive transfer on day 5 p.i.

$CD8^+$ T-cell expansion is thought to be initiated in the cervical lymph nodes, the major site of T-cell priming during CNS infections, and then expansion continues in the spleen, followed by rapid accumulation of virus-specific T cells in the CNS during MHV infection (17). Norbury et al. showed that virus-specific $CD8^+$ T cells are primed by dendritic cells, but not macrophages, in vivo after infection with vaccinia virus (20). We do not know which antigen-presenting cells are responsible for priming naive $CD8^+$ T cells after MHV infection of the CNS. Analysis of splenocytes on days 10 and 12 p.i. revealed the presence of transferred P14 cells in this organ in all transfer recipients regardless of the day p.i. on which the cells were transferred (data not shown), although the percentage of activated spleen-derived P14 cells was dependent upon the day of transfer. $CD8^+$ $CD45.2^+$ T cells were present in the spleens of both transfer groups (days 3 and 5 p.i.); however, only cells harvested from mice that received the transfer on day 3 p.i. secreted IFN-γ in response to gp33 peptide (data not shown), which suggests that failure of the day 5 p.i. transfer to become activated was due to a deficit in priming.

The increased virus-specific $CD8^+$ T-cell response observed in protected mice limited virus replication and spread within the CNS of RA59-gfp/gp33-infected animals. At day 5 p.i., virus titers and viral antigen staining were reduced in these animals. In some CNS infections, such as Borna disease virus and i.c. infection of mice with LCMV, $CD8^+$ T cells can play a detrimental role during the infection; however, virus-specific $CD8^+$ T cells primarily control virus replication and protect against virus spread, CNS damage, and encephalitis in MHV strain A59-infected mice (2, 4). Thus, during the acute phase of MHV infection of the CNS, virus-specific $CD8^+$ T cells play a crucial role in protection from both acute and chronic disease and a stronger $CD8^+$ T-cell response is beneficial to the host.

Virus antigen was detected throughout the brain and in the gray and white matter of the spinal cord with similar kinetics, peaking on day 5 p.i. and diminishing by day 7 p.i. Virus antigen was still detected in the spinal cords on day 7 p.i. but was present only in the white matter. On the basis of studies of JHM, virus spread from the brain into the spinal cord is thought to occur in a retrograde fashion via transneuronal spread; the rapid appearance of virus in the spinal cord, as observed here, is consistent with this. Whether the $CD8^+$ T-cell-mediated block in virus spread to the spinal cord reflected an overall diminished load of virus within the CNS or whether $CD8^+$ T cells mediated clearance of particular cell types is not known.

Clearance of infectious virus from the CNS requires both perforin- and cytokine-mediated mechanisms. Interestingly, our vaccination studies with perforin-deficient mice with recombinant *L. monocytogenes* expressing the gp33 epitope, followed by a challenge with RA59-gfp/gp33, revealed that perforin was necessary for protection, as determined by virus titers in the brain (5). This is interesting since the majority of A59-infected cells are positive for the neuronal marker dendrite-specific microtubule-associated protein 2 (25). Perforin is required for clearance from microglia and astrocytes, which express major histocompatibility complex class I; thus, these cell types may support the majority of virus replication. It is unclear how adoptively transferred P14 $CD8^+$ T cells mediated protection from virus spread via transneuronal pathways, but it likely involved cytokine-mediated effects and is of current interest.

Interestingly, we found that the retention of IFN-γ-secreting gp33-specific $CD8^+$ T cells at 4 weeks p.i. was similar in all RA59-gfp/gp33-infected animals regardless of transfer of gp33-specific $CD8^+$ T cells or the amount of virus replication and spread that occurred during the acute phase of infection. In addition, both recipients and nonrecipients had similar percentages of S598-specific $CD8^+$ T cells despite having very different levels of S598-specific $CD8^+$ T cells at the peak of infiltration during the acute phase of infection. Thus, the level of replication and spread during the acute phase of infection appeared to have little if any effect on the retention of $CD8^+$ T cells during the chronic phase of infection. It has been shown in several viral infections of the CNS that $CD8^+$ T cells are maintained within the brain after the acute phase of infection is resolved (11, 32). The function of these retained virus-specific $CD8^+$ T cells is not clear, but as van der Most et al. (32) suggest in a model of dengue virus infection of the mouse CNS, the brain may retain local, activated, virus-specific $CD8^+$ T cells with an effector memory phenotype as an in situ rapid response force.

Factors contributing to the maintenance of virus-specific $CD8^+$ T cells in the CNS are also largely unknown. Retention of $CD8^+$ T cells within the CNS of JHM-infected animals is thought to be largely dependent on the presence of viral RNA and possibly very low levels of antigen expression (16). In JHM-infected mice that recognize both $H\text{-}2D^b$- and $H\text{-}2D^d$-restricted epitopes, the epitope specificity of $CD8^+$ T cells changes from the acute to the chronic phase of infection with a decrease in $H\text{-}2D^d$-restricted nucleocapsid-specific $CD8^+$ T cells and an increase in $H\text{-}2D^b$ spike-specific $CD8^+$ T cells suggestive of altered antigen presentation during the chronic phase of infection (1). However, in the present study animals that were protected from acute disease via adoptive transfer exhibited minimal virus replication and spread, and although possible, it is unlikely that persistent viral RNA was maintaining the population of activated $CD8^+$ T cells in these mice.

The severity of demyelination in the chronic phase of infection did not correspond to the levels of activated virus-specific $CD8^+$ T cells. At 4 weeks p.i., total numbers and percentages of epitope-specific $CD8^+$ T cells in the brain were similar in transfer recipients and nonrecipients infected with either RA59-gfp/gp33 or RA59-gfp. However, demyelination was much less severe in animals protected from virus replication and spread, P14 splenocyte recipients infected with RA59-gfp/

gp33, despite a strong immune response during the acute phase of infection. This supports previous findings that CD8$^+$ T cells likely do not play a direct role in the process of demyelination (9, 15, 30).

The outcome of the acute stage of A59-induced CNS disease depends on the rapid recruitment and activation of CD8$^+$ T cells, and a good prognosis is linked with limited spread of the virus within the CNS, specifically to the spinal cord. Preventing virus spread to the spinal cord reduced levels of demyelination seen in the chronic stage of disease, suggesting that the presence of viral RNA and/or low levels of viral antigen are required for demyelination to occur. This study also demonstrated that the initial priming event after infection with a neurotropic pathogen was critical in establishing a long-lasting protective immune response in the brain. Thus, the immediate host immune response is critical and determines the outcome of A59 infection.

ACKNOWLEDGMENTS

This work was supported by NIH grants AI 47800, AI 60021, NS 30606 (S.R.W.), and AI 45025 (H.S.), and K.C.M. was supported by NIH training grant AI 007324.

We thank Devon J. Shedlock and Lauren A. Zenewicz for providing P14 mice.

REFERENCES

1. **Bergmann, C. C., J. D. Altman, D. Hinton, and S. A. Stohlman.** 1999. Inverted immunodominance and impaired cytolytic function of CD8$^+$ T cells during viral persistence in the central nervous system. J. Immunol. **163:**3379–3387.
2. **Bilzer, T., and L. Stitz.** 1994. Immune-mediated brain atrophy. CD8$^+$ T cells contribute to tissue destruction during Borna disease. J. Immunol. **153:**818–823.
3. **Brandle, D., K. Burki, V. A. Wallace, U. H. Rohrer, T. W. Mak, B. Malissen, H. Hengartner, and H. Pircher.** 1991. Involvement of both T cell receptor V alpha and V beta variable region domains and alpha chain junctional region in viral antigen recognition. Eur. J. Immunol. **21:**2195–2202.
4. **Buchmeier, M. J., R. M. Welsh, F. J. Dutko, and M. B. Oldstone.** 1980. The virology and immunobiology of lymphocytic choriomeningitis virus infection. Adv. Immunol. **30:**275–331.
5. **Chua, M., K. MacNamara, L. SanMateo, H. Shen, and S. R. Weiss.** 2004. Effects of an epitope-specific CD8$^+$ T-cell response on murine coronavirus central nervous system disease: protection from virus replication and antigen spread and selection of epitope escape mutants. J. Virol. **78:**1150–1159.
6. **DasSarma, J., E. Scheen, S.-H. Seo, M. Koval, and S. R. Weiss.** 2002. Enhanced green fluorescent protein expression may be used to monitor murine coronavirus spread in vitro and in the mouse central nervous system. J. Neurovirol. **8:**1–11.
7. **Drosten, C., S. Gunther, W. Preiser, S. van der Werf, H. R. Brodt, S. Becker, H. Rabenau, M. Panning, L. Kolesnikova, R. A. Fouchier, A. Berger, A. M. Burguiere, J. Cinatl, M. Eickmann, N. Escriou, K. Grywna, S. Kramme, J. C. Manuguerra, S. Muller, V. Rickerts, M. Sturmer, S. Vieth, H. D. Klenk, A. D. Osterhaus, H. Schmitz, and H. W. Doerr.** 2003. Identification of a novel coronavirus in patients with severe acute respiratory syndrome. N. Engl. J. Med. **348:**1967–1976.
8. **Fleming, J. O., J. J. Houtman, H. Alaca, D. Hinze, D. McKenzie, J. Aiken, T. Bleasdale, and S. Baker.** 1993. Persistence of viral RNA in the central nervous system of mice inoculated with MHV-4. Adv. Exp. Med. Biol. **342:**327–332.
9. **Gombold, J., R. M. Sutherland, E. Lavi, Y. Paterson, and S. R. Weiss.** 1995. Mouse hepatitis virus A59-induced demyelination can occur in the absence of CD8$^+$ T cells. Microb. Pathog. **18:**211–221.
10. **Haring, J. S., L. L. Pewe, and S. Perlman.** 2002. Bystander CD8 T cell-mediated demyelination after viral infection of the central nervous system. J. Immunol. **169:**1550–1555.
11. **Hawke, S., P. G. Stevenson, S. Freeman, and C. R. Bangham.** 1998. Long-term persistence of activated cytotoxic T lymphocytes after viral infection of the central nervous system. J. Exp. Med. **187:**1575–1582.
12. **Hingley, S. T., J. L. Gombold, E. Lavi, and S. R. Weiss.** 1994. MHV-A59 fusion mutants are attenuated and display altered hepatotropism. Virology **200:**1–10.
13. **Houtman, J. J., and J. O. Fleming.** 1996. Pathogenesis of mouse hepatitis virus-induced demyelination. J. Neurovirol. **2:**361–376.
14. **Lavi, E., P. S. Fishman, M. K. Highkin, and S. R. Weiss.** 1988. Limbic encephalitis after inhalation of a murine coronavirus. Lab. Investig. **58:**31–36.
15. **Marten, N. W., S. A. Stohlman, R. D. Atkinson, D. R. Hinton, J. O. Fleming, and C. C. Bergmann.** 2000. Contributions of CD8$^+$ T cells and viral spread to demyelinating disease. J. Immunol. **164:**4080–4088.
16. **Marten, N. W., S. A. Stohlman, and C. C. Bergmann.** 2000. Role of viral persistence in retaining CD8$^+$ T cells within the central nervous system. J. Virol. **74:**7903–7910.
17. **Marten, N. W., S. A. Stohlman, J. Zhou, and C. C. Bergmann.** 2003. Kinetics of virus-specific CD8$^+$ T-cell expansion and trafficking following central nervous system infection. J. Virol. **77:**2775–2778.
18. **Matthews, A. E., E. Lavi, S. R. Weiss, and Y. Paterson.** 2002. Neither B cells nor T cells are required for CNS demyelination in mice persistently infected with MHV-A59. J. Neurovirol. **8:**257–264.
19. **Murali-Krishna, K., J. D. Altman, M. Suresh, D. J. Sourdive, A. J. Zajac, J. D. Miller, J. Slansky, and R. Ahmed.** 1998. Counting antigen-specific CD8 T cells: a reevaluation of bystander activation during viral infection. Immunity **8:**177–187.
20. **Norbury, C. C., D. Malide, J. S. Gibbs, J. R. Bennink, and J. W. Yewdell.** 2002. Visualizing priming of virus-specific CD8$^+$ T cells by infected dendritic cells in vivo. Nat. Immunol. **3:**265–271.
21. **Ontiveros, E., L. Kuo, P. S. Masters, and S. Perlman.** 2001. Inactivation of expression of gene 4 of mouse hepatitis virus strain JHM does not affect virulence in the murine CNS. Virology **289:**230–238.
22. **Parra, B., D. R. Hinton, N. W. Marten, C. C. Bergmann, M. T. Lin, C. S. Yang, and S. A. Stohlman.** 1999. IFN-γ is required for viral clearance from central nervous system oligodendroglia. J. Immunol. **162:**1641–1647.
23. **Perlman, S., G. Jacobsen, and A. Afifi.** 1989. Spread of a neurotropic murine coronavirus into the CNS via the trigeminal and olfactory nerves. Virology **170:**556–560.
24. **Pewe, L., S. B. Heard, C. Bergmann, M. O. Dailey, and S. Perlman.** 1999. Selection of CTL escape mutants in mice infected with a neurotropic coronavirus: quantitative estimate of TCR diversity in the infected central nervous system. J. Immunol. **163:**6106–6113.
25. **Phillips, J. J., M. M. Chua, G. F. Rall, and S. R. Weiss.** 2002. Murine coronavirus spike glycoprotein mediates degree of viral spread, inflammation, and virus-induced immunopathology in the central nervous system. Virology **301:**109–120.
26. **Stohlman, S. A., C. C. Bergmann, D. J. Cua, M. T. Lin, S. Ho, W. Wei, and D. R. Hinton.** 1998. Apoptosis of JHMV-specific CTL in the CNS in the absence of CD4$^+$ T cells. Adv. Exp. Med. Biol. **440:**425–430.
27. **Stohlman, S. A., C. C. Bergmann, M. T. Lin, D. J. Cua, and D. R. Hinton.** 1998. CTL effector function within the central nervous system requires CD4$^+$ T cells. J. Immunol. **160:**2896–2904.
28. **Stohlman, S. A., C. C. Bergmann, R. C. van der Veen, and D. R. Hinton.** 1995. Mouse hepatitis virus-specific cytotoxic T lymphocytes protect from lethal infection without eliminating virus from the central nervous system. J. Virol. **69:**684–694.
29. **Sussman, M. A., R. A. Shubin, S. Kyuwa, and S. A. Stohlman.** 1989. T-cell-mediated clearance of mouse hepatitis virus strain JHM from the central nervous system. J. Virol. **63:**3051–3056.
30. **Sutherland, R. M., M. M. Chua, E. Lavi, S. R. Weiss, and Y. Paterson.** 1997. CD4$^+$ and CD8$^+$ T cells are not major effectors of mouse hepatitis virus A59-induced demyelinating disease. J. Neurovirol. **3:**225–228.
31. **Tsai, J. C., L. de Groot, J. D. Pinon, K. T. Iacono, J. J. Phillips, S. H. Seo, E. Lavi, and S. R. Weiss.** 2003. Amino acid substitutions within the heptad repeat domain 1 of murine coronavirus spike protein restrict viral antigen spread in the central nervous system. Virology **312:**369–380.
32. **van der Most, R. G., K. Murali-Krishna, and R. Ahmed.** 2003. Prolonged presence of effector-memory CD8 T cells in the central nervous system after dengue virus encephalitis. Int. Immunol. **15:**119–125.
33. **Wang, F. I., S. A. Stohlman, and J. O. Fleming.** 1990. Demyelination induced by murine hepatitis virus JHM strain (MHV-4) is immunologically mediated. J. Neuroimmunol. **30:**31–41.
34. **Wong, P., and E. G. Pamer.** 2003. Feedback regulation of pathogen-specific T cell priming. Immunity **18:**499–511.
35. **Wu, G. F., A. A. Dandekar, L. Pewe, and S. Perlman.** 2000. CD4 and CD8 T cells have redundant but not identical roles in virus-induced demyelination. J. Immunol. **165:**2278–2286.